

## MAGNETICALLY SENSITIVE CARBON-BASED NANOCOMPOSITES FOR THE REMOVAL OF DYES AND HEAVY METALS FROM WASTEWATER: A REVIEW

Nazar Nahurskyi<sup>1</sup>, ✉, Myroslav Malovanyy<sup>1</sup>, Ihor Bordun<sup>1</sup>, Ewelina Szymczykiewicz<sup>2</sup>

<https://doi.org/10.23939/chcht18.02.170>

**Abstract.** The methods of wastewater treatment from heavy metal ions and dyes are analyzed, and the key advantages of powdered magnetically sensitive carbon nanocomposites as adsorbents are shown. Methods for selecting and preparing raw materials and activators for the synthesis of such nanocomposites are considered, and methods for synthesizing nanocomposites are analyzed. The properties, modeling of adsorption kinetics and isotherms, and efficiency of magnetic carbon nanocomposites for wastewater treatment from dyes and heavy metals are described.

**Keywords:** adsorption, carbon nanocomposite, magnetically sensitive adsorbent, wastewater treatment, heavy metals, dyes.

### 1. Introduction

Water is the basic resource for life on Earth, and access to clean water is crucial for humans and ecosystems. However, in recent decades, water quality has been adversely affected by continuous population growth, rapid industrialization, increasing urbanization, and careless use of natural resources.<sup>1-3</sup> Excessive discharges of untreated wastewater from non-ferrous metal-based industries, and wastewater containing dyes from the textile, pulp and paper, fertilizer, paint, and pigment industries are among the main sources of water pollution.

It should be added that about 10,000 different commercial dyes and pigments are used in industrial production.<sup>4</sup> This requires the search for and development of certain universal approaches to wastewater treatment in such industries. Heavy metal ions are very dangerous because of their toxic and carcinogenic effects. Some of them, such as lead (Pb), arsenic (As), mercury (Hg),

chromium (Cr), especially hexavalent chromium, nickel (Ni), barium (Ba), cadmium (Cd), cobalt (Co), vanadium (V), *etc.*, are particularly dangerous and show toxicity even at extremely low concentrations (in the ppb range).<sup>5</sup> Also, some metal ions are not biodegradable or biotransformable and thus persist and accumulate in the environment for a long time.

This study aimed to systematize the data obtained by various researchers in recent years on the synthesis and effectiveness of magnetically sensitive carbon composites for wastewater treatment from pollutants such as dyes and heavy metal ions.

### 2. Characterization of Methods for Removing Heavy Metals and Dyes from Wastewater

Wastewater treatment typically requires a combination of physical, chemical and biochemical treatment. These methods include adsorption, chemical precipitation, membrane filtration, ion exchange, electrolysis, coagulation, solvent extraction, reverse osmosis, electrocoagulation, *etc.* A brief list of methods for removing pollutants from wastewater, as well as their advantages and disadvantages are given in Table 1.

As shown in Table 1, most of these methods have their advantages and limitations. The main disadvantages are incomplete removal of contaminants, low selectivity, high reagent and chemical requirements, high energy consumption, and the generation of other toxic wastes. Another factor that negatively affects even effective purification methods is the high cost of their application. Since the magnetically sensitive carbon composites we consider in this article are most often used as adsorbents for various types of pollution, the following analysis will focus on adsorption processes.

Adsorption processes are attractive approaches to wastewater treatment, particularly because the adsorbent is inexpensive, does not require pre-treatment before use, and is

<sup>1</sup> Lviv Polytechnic National University 12, S. Bandery St., Lviv 79013, Ukraine

<sup>2</sup> Czestochowa University of Technology 69, Dabrowskiego str., Czestochowa 42-201, Poland

✉ [nazar.o.nahurskyi@lpnu.ua](mailto:nazar.o.nahurskyi@lpnu.ua)

© Nahurskyi N., Malovanyy M., Bordun I., Szymczykiewicz E., 2024

easy to regenerate. Adsorption, despite the problems associated with adsorbent disposal and additional pollution from adsorbents, is an efficient and simple process that has low operating costs, and high removal capacity. It is easy to implement and relatively free of undesirable by-products.<sup>7,11,12</sup>

Adsorption processes are attractive approaches to wastewater treatment, particularly because the adsorbent

is inexpensive, does not require pre-treatment before use, and is easy to regenerate. Adsorption, despite the problems associated with adsorbent disposal and additional pollution from adsorbents, is an efficient and simple process that has low operating costs, and high removal capacity. It is easy to implement and relatively free of undesirable by-products.<sup>7,11,12</sup>

**Table 1.** Methods of dye and heavy metal removal, their advantages and disadvantages.<sup>6-10</sup>

| Methods    |   | Advantages  | Disadvantages  |
|------------|---|---|--|
| Physical   | Adsorption                              | High sorption capacity, wide pH range, ease of use, flexibility and simple design                 | High cost of adsorbent, difficult separation, small surface area, low selectivity                    |
|            | Membrane filtration                     | Effective for all types of dyes, high separation selectivity, low space requirement, low pressure | Sludge production, only suitable for small cleaning volumes, high maintenance and operating costs    |
|            | Nanofiltration                          | High separation efficiency, ease of operation, reliability  | Complexity of operation  |
|            | Ion exchange                            | No sorbent loss, material regeneration, selectivity   | High cost, low efficiency for dispersed dyes, availability for limited number of metal ions          |
|            | Coagulation and flocculation            | Cost-effective  | Sludge production, post coagulation treatment requirements, e.g. flocculation, chemical requirements |
|            | Electroflotation and electrocoagulation | Selectivity to metal ions, no use of chemicals, efficiency  | High current density requirements, high operating and capital costs                                  |
|            | Electrodialysis                         | Increased selectivity   | High operating costs due to energy consumption and membrane contamination                            |
| Chemical   | Fenton's reagents                       | Effective decolouration, low cost of reagents   | Sludge production  |
|            | Ozonation                               | Effective discolouration  | High operating costs   |
|            | Photocatalysis                          | Simultaneous removal of metals and organic pollutants, low operating costs                        | Production of toxic by-products, duration of purification  |
|            | Adsorption                              | Strong chemical bonds   | Agglomeration, low permeability and poor mass transfer   |
|            | Chemical deposition                     | Low cost, environmentally friendly operation  | Production of large amounts of sludge  |
| Biological | Aerobic degradation                     | Low operating costs, effective for azo dye removal  | Slow process, need for a favourable environment for microbial growth                                 |
|            | Biosorption                             | Simple operation, low operating costs, high efficiency, biosorbent regeneration                   | High dependence on environmental conditions  |

Adsorbents traditionally used for water treatment include activated carbon (AC), clay minerals, silica gel, and zeolites. However, due to their high production costs, the focus of researchers has shifted to environmentally friendly materials, including biomaterials. The most promising adsorbent is AC. It has high adsorption efficiency, large specific surface area and volume, and high surface reactivity.<sup>13,14</sup>

Modern industrial adsorbents are typically used in two forms: granular and powder. Granular adsorbents have the advantage that they are easy to load into adsorption columns and do not need to be separated from the solution. However, the large particle size results in

reduced kinetic properties of such adsorbents, and the granulation process not only negatively affects the adsorption properties, but also increases the cost of the adsorbent itself. In this regard, powder adsorbents look more promising. In this case, a new problem arises: separation of adsorbent from solution. Due to its small particle size and density, which is comparable to the density of water, it is difficult to separate the powder adsorbent by settling. In such cases, a filtering process is used, but this is a quite slow process. Moreover, the filters become clogged and some of the adsorbent is lost. One way out of this situation is the synthesis of magnetically sensitive adsorbents that can be easily separated from the

aqueous medium by magnetic separation, while the adsorption capacity of such adsorbents remains at a high level. First of all, such adsorbents are suitable for wastewater treatment of heavy metal ions and dyes.<sup>7,15,16</sup>

### 3. Magnetically Sensitive Adsorbents and Methods of Their Synthesis

Magnetic separation is based on the fact that magnetic nanoparticles can be manipulated by an external magnetic field gradient. To achieve effective magnetic separation of micrometric or nanoscale materials from a viscous medium, the magnetic force generated by the external magnetic field must overcome the resistive force associated with the supporting fluid. Larger magnetic particles have a higher magnetic susceptibility, which results in higher extraction rates from the aqueous medium. In other words, larger particles are more effective for magnetic separation. However, for adsorption applications, smaller magnetic particles (nanoparticles) or nanocomposites with a certain content of magnetically sensitive nanoparticles in a porous matrix are preferred due to their high surface area-to-volume ratio.<sup>17,18</sup>

Magnetic nanocomposites have attracted increasing attention in recent decades for use as sorbents in water treatment processes.<sup>19-23</sup> Magnetic nanocomposites are multi-phase materials in which at least one of the constituent phases is a magnetic nanoparticle. In general, a magnetic nanocomposite is prepared by embedding magnetic nanoparticles into various materials such as polymers, silica, and carbon,<sup>24</sup> which are called matrices. Nanocomposites can combine the advantages of two or more materials with different physical and chemical properties, making them promising for use in many processes, including water and wastewater treatment.<sup>25,26</sup>

The most common metallic nanoparticles used to prepare magnetic materials are nickel, cobalt, and iron.<sup>27-29</sup> Nevertheless, iron compounds are commonly utilized due to their low cost and magnetic characteristics. Siddiqui *et al.*<sup>27</sup> have reviewed the main sources of iron and they comprise ferrous sulfate  $\text{FeSO}_4$ , ferric nitrate  $\text{Fe}(\text{NO}_3)_3$ , ferric oxide  $\text{Fe}_2\text{O}_3$ , ferrous ferric oxide  $\text{Fe}_3\text{O}_4$ , ferric chloride  $\text{FeCl}_3$  and iron ores like magnetite and maghemite. As mentioned by Meng *et al.*,<sup>30</sup> the iron compounds display numerous advantages: they can be used to modify supports at low temperatures (around 180 °C), they have low toxicity for ecosystems and human health thus being safe and environmentally friendly, and they also offer physical stability to supports and good magnetic performance. These characteristics can be exploited in water purification and treatment.

Magnetic nanoparticles can be incorporated into inorganic or organic matrices,<sup>31,32</sup> depending on the

characteristics of the material used.<sup>33</sup> For example, magnetic nanoparticles can be coated by a coating agent, e.g. silica, or dispersed in the pores of a carbonaceous material, e.g. activated carbon.<sup>34</sup> Fig. 1 illustrates the structure of some typical magnetic nanocomposites. In some cases, to obtain higher stability, magnetic nanoparticles or magnetic nanoparticles matrix can be functionalized. In many works, functionalization is performed by the insertion of amino groups.<sup>35-41</sup>

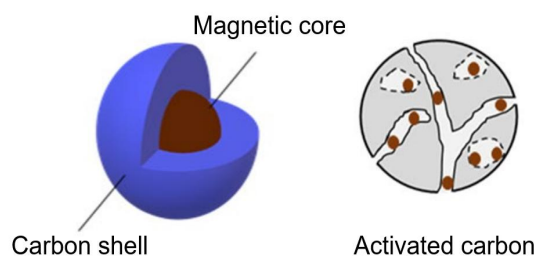


**Fig. 1.** Typical iron-based magnetic nanocomposites that can be synthesized by embedding magnetic nanoparticles in various carbon materials<sup>42</sup>

Different approaches to the preparation of magnetic nanocomposites are described in the literature. The core-shell structure nanocomposites are prepared by encapsulating the magnetic nanoparticles in a matrix, that acts as a coating for the magnetic core.<sup>43,44</sup> Alternatively, core-shell type nanocomposites can be prepared *via* layer-by-layer coating, in which the magnetic nanoparticles are functionalized and subsequently coated.<sup>44</sup> For non-core-shell structure nanocomposites, the most used technique is the mixing of magnetic nanoparticles with the matrix under the influence of sonication to prevent aggregation. The magnetic nanoparticles can be synthesized separately and then mixed with the matrix or synthesized together with the matrix.<sup>33,45</sup>

#### 3.1. Synthesis of Carbon-Based Magnetic Adsorbents

Several methods have been used to synthesize magnetic carbon nanocomposites, and practically each synthesis route applies more than two stages for obtaining the final material. Synthesis technologies may differ depending on the carbon source nature, but all approaches generally include impregnation with iron salts and chemical co-precipitation of iron oxide nanoparticles.

Generally, various stages are necessary to produce magnetic activated carbon and biochar (BC). First, the carbonization of a precursor is required, and it can be performed by traditional pyrolysis or hydrothermal method. In the second stage, the impregnation with iron phases in a liquid phase is performed to modify AC or

BC. Alternatively, the iron salts can be mixed with a carbon precursor and then the carbonization step is carried out.<sup>46,47</sup>

In the direct synthesis, an impregnation stage is required, where the support precursor (*e.g.*, lignocellulosic biomass) is mixed with iron salts or iron phases. Then, the pyrolysis or hydrothermal stage is performed to obtain magnetic BC or hydrochar (HC). Otherwise, the first stage of an indirect synthesis is the precursor carbonization, and, once BC or HC has been obtained, the second stage consists of carbon-based material impregnation with a

magnetic phase of iron oxides to obtain magnetic BC or HC. These procedures are illustrated in Fig. 2.

The direct synthesis of magnetic AC involves the addition of chemicals at the impregnation stage and activation at the subsequent carbonization stage by hydrothermal treatment or pyrolysis, as shown in Fig. 3. Note that the production of magnetic AC by indirect synthesis depends on the activation step, which can be performed after carbonization by chemical and/or physical means, followed by impregnation to incorporate magnetic species.

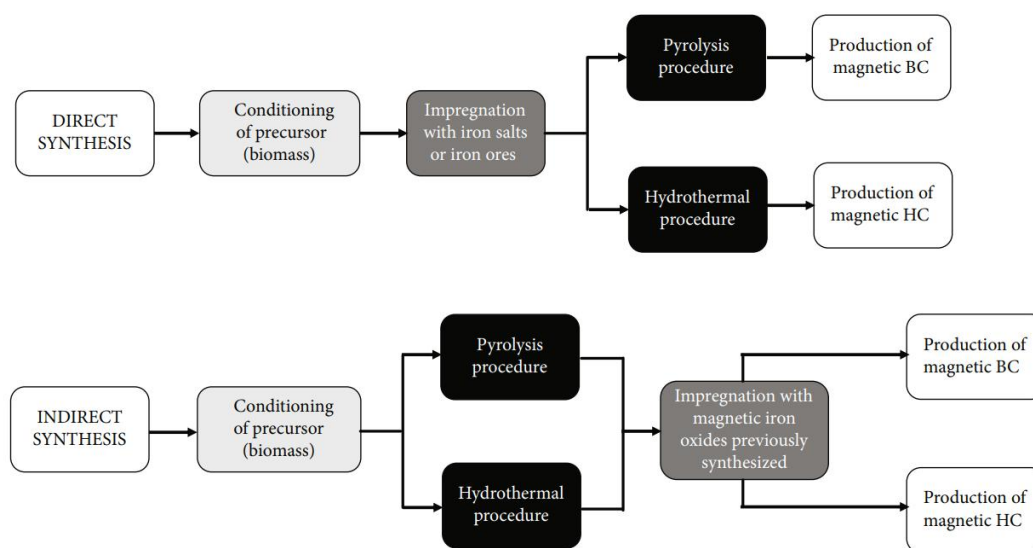


**Fig. 2.** General steps for the preparation of magnetic hydrochar (HC) and magnetic biochar (BC) by direct or indirect synthesis<sup>47</sup>

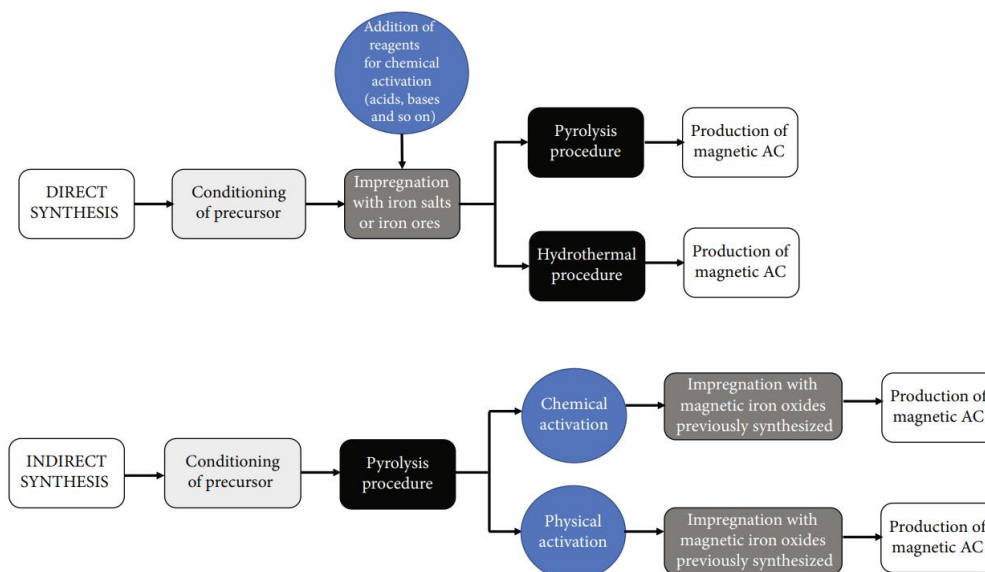


**Fig. 3.** General steps for the preparation of magnetic activated carbon (AC) by direct or indirect synthesis.<sup>47</sup>

A relevant advantage of the synthesis of AC, HC, and BC, as carbon-based supports, is the use of low-cost raw materials as precursors. In this sense, researchers have prepared AC and BC using biomass sources with non-commercial value like rice husks,<sup>48</sup> pineapple crown leaf waste,<sup>49</sup> pistachio shells,<sup>50</sup> pomelo peels,<sup>51</sup> beet pulp and corn stalks,<sup>52</sup> and many others. Also, alternative carbon sources like industrial and urban residues (e.g., Tetra pack, PET bottles, and tires) can be utilized to obtain these carbon supports.<sup>53-55</sup> Once the precursor for the carbon matrix preparation has been selected and acondicionated (this stage generally includes washing, particle size reduction, and pretreatment), the carbonization stage is the next step. Note that several methods can be chosen for biomass carbonization, the most common of which are pyrolysis and hydrothermal carbonization.

Pyrolysis involves the formation of a low-developed porous solid matrix (usually called a char), where the precursor is submitted to a thermal treatment without oxygen at temperatures from 500 to 1000 °C.<sup>56,57</sup> This char can be also obtained *via* thermal treatment under the presence of oxygen, and this process is commonly referred as carbonization.<sup>58,59</sup> For BC and char production, pyrolysis or carbonization is the only stage employed in the preparation route, but an additional activation stage is needed to obtain AC, which can involve the use of different (physical or chemical) reagents. For example, carbon dioxide or water vapor at a temperature of 600-

1200 °C are typical physical activators that cause the formation of the AC well-developed porous structure.<sup>58,59</sup>

On the other hand, hydrothermal carbonization (HTC) is the thermochemical conversion process that transforms biomass under the presence of pressurized water (at subcritical conditions) into a carbon-based material usually referred as HC (i.e., hydrochar).<sup>60</sup> This process is regarded as a green route to prepare new materials from biomasses and other feedstocks in a closed reactor or autoclave under the presence of water at low temperatures (150-250 °C). Compared to traditional heat treatment, HTC has a number of advantages, as it not only helps to generate a surface rich in functional groups but also involves reduced energy consumption and low cost. Raw HC obtained at common operating conditions has a low specific surface area (<100 m<sup>2</sup>/g), but contains a significant amount of oxygenated functionalities if water is the reaction medium to prepare this adsorbent.<sup>30,61-64</sup> For example, Cai *et al.*<sup>65</sup> reported the preparation of a magnetic BC for chromium adsorption using peanut shells, deionized water, hexamethylenediamine, and FeCl<sub>3</sub>·6H<sub>2</sub>O. The adsorbent was obtained *via* HTC at 220 °C for 12 h. The maximum adsorption capacity of this magnetic material was 142.86 mg/g and could be reused in 3 removal cycles. Fig. 4 illustrates the methodology used to produce magnetic BC from peanut shells.<sup>65</sup> Note that HC with high surface area and porosity can be prepared if a postactivation step is performed.

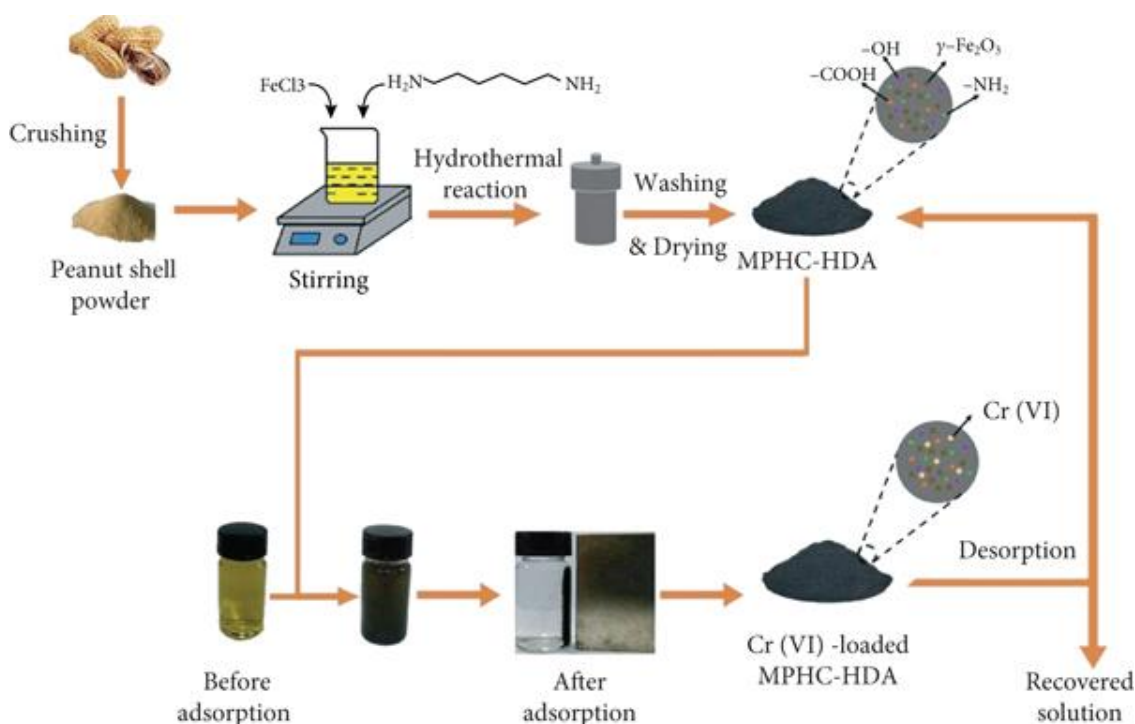


Fig. 4. HTC used to prepare magnetic adsorbents for Cr (VI) removal from aqueous solution.<sup>65</sup>

Herein, it is convenient to highlight that alternative technologies can be utilized to prepare the carbon-based support, and they include the application of microwave and plasma.<sup>59,66</sup> For instance, the main objective of microwave-assisted pyrolysis is to reduce the preparation time and to enhance the adsorption properties of the solid matrix.<sup>59</sup> In microwave instruments, the precursor pyrolysis/carbonization and adsorbent activation can be carried out. This technology ensures a uniform heating process, which allows the homogenization of the bulk properties of the final product.<sup>59</sup> Microwave power and radiation time can impact the char textural parameters like surface area and pore volume.<sup>67</sup>

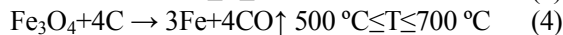
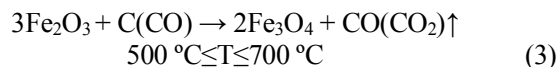
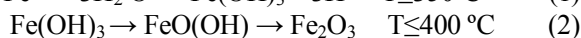
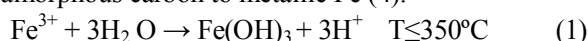
As noted, another important step is impregnation with magnetic salts to impart magnetic properties to the BC, AC, or HC. This task can be accomplished with the help of:

- non-magnetic iron oxides (*e.g.*, hematite and goethite) or iron salts, which can be mixed with the carbonaceous precursor before its carbonization in aqueous solution at a predetermined temperature and time to ensure its impregnation. The impregnated precursor can be carbonized to directly obtain the magnetic adsorbents.

- char or AC, which can be mixed with magnetic salts in an aqueous solution (or chemical synthesis of magnetic iron oxide using, for example, sol-gel or co-precipitation methods, or physical mixing of magnetic iron oxides previously synthesized by thermal decomposition, chemical reduction, sol-gel or co-precipitation can be used for impregnation).<sup>59</sup>

The final magnetic material could acquire different structural, chemical, and physical characteristics depending on the preparation conditions. For instance, the precursor (biomass or other carbon source), temperature, and impregnation ratio could have a significant impact on the final adsorbent properties.

During the carbonization process of raw materials in the presence of iron salts, various processes take place that lead to the formation of iron oxides and the development of porosity.<sup>68,69</sup> For example, when FeCl<sub>3</sub> is used as an activator, the following transformations take place depending on the process temperature. The Fe<sup>3+</sup> ion is hydrolyzed to Fe(OH)<sub>3</sub> at 350 °C (1). Further heating in an inert atmosphere leads to dehydration and conversion of the hydroxide to Fe<sub>2</sub>O<sub>3</sub> haematite at 400 °C (2). At higher temperatures (from 500 °C to 700 °C) Fe<sub>2</sub>O<sub>3</sub> haematite is reduced to Fe<sub>3</sub>O<sub>4</sub> magnetite by amorphous carbon and CO gas (3). By selecting the intensity of the inert gas jet (*e.g.*, argon) it is possible to ensure continuous removal of CO and CO<sub>2</sub> reaction products as they are formed. Fe<sub>3</sub>O<sub>4</sub> magnetite can be further reduced with amorphous carbon to metallic Fe (4).



Several studies<sup>70,71</sup> have reported that FeCl<sub>3</sub> additionally promotes pore development in carbonaceous materials. Unfortunately, the mechanism of FeCl<sub>3</sub> activation is not well understood. On the other hand, the two reduction reactions given in equations (3) and (4) may contribute to the development of pores in magnetic sorbent samples by converting C to CO and removing carbon in the form of CO, resulting in certain cavities within the material structure.

It should be noted that the adsorption capacity of carbon nanocomposites with Fe<sub>3</sub>O<sub>4</sub> is significantly lower than that of their non-magnetic forms when recalculated on the total weight of the adsorbent.<sup>48,72,73</sup> However, most of the magnetic adsorbent mass is magnetite, which has weak sorption properties. Therefore, to assess the "real" efficiency of carbon adsorbents, the adsorption capacity was expressed relative to the weight of BC or AC in the composite.<sup>74</sup> In this study, the specific surface area was 75.4 (the relative surface area was 301.6, surface area before magnetization was 319.1) and 90.6 (the relative surface area was 362.4, surface area before magnetization was 544.9) for AC and BC, respectively, *i.e.* the relative surface area does not decrease significantly.

## 4. Adsorption Properties of Magnetically Sensitive Sorbents for Heavy Metals and Dyes

As mentioned above, the adsorption separation process is one of the most widely used technologies in wastewater treatment due to its ease of operation, flexibility and high efficiency.<sup>31</sup> Several kinetic and isothermal models are used to evaluate the adsorbent efficiency.<sup>32</sup> The most commonly used are the equilibrium isotherms developed by Langmuir and Freundlich and the Lagerhren equation for kinetic studies, known as pseudo-first-order and pseudo-second-order.<sup>23</sup>

Various pollutants, including dyes, heavy metals, and polycyclic aromatic compounds (PAHs), can be removed by magnetic sorbents through adsorption, oxidation, and reduction processes.<sup>75</sup> Zhang *et al.*<sup>76</sup> suggested that the heavy metal ions of Cr(VI) were firstly adsorbed on the surface of magnetic biosorbents derived from *Melia azedarach* wood, and eventually reduced to Cr(III) ions. Furthermore, pyrene was oxidized and degraded by persulfate that was activated by the composite of Fe<sub>3</sub>O<sub>4</sub> supported on bamboo biomass.<sup>77</sup>

**Table 2.** Magnetically sensitive adsorbents, methods of their synthesis, adsorption properties for heavy metals and dyes

| Matrix                     | Modification agent                                 | Synthesis method  | Saturation magnetization (emu/g) | Specific surface area (m <sup>2</sup> /g) | Target pollutant | Adsorption test conditions (pH/time) | Maximum adsorption capacity (mg/g) | Isotherm model   | Kinetic model | Ref. |
|----------------------------|--|---|----------------------------------|---|------------------|--------------------------------------|------------------------------------|------------------|---------------|------|
| 1                          | 2  | 3   | 4                                | 5   | 6                | 7                                    | 8                                  | 9                | 10            | 11   |
| Peach gum                  | Fe <sub>3</sub> O <sub>4</sub>                     | Simultaneous formation of magnetic nanoparticles and cross-linking of peach gum                       | 10,8                             | –   | Methylene blue   | 7/1 h                                | 231,5                              | Langmuir         | PSO           | 78   |
| Sorghum husks              | Fe <sub>3</sub> O <sub>4</sub>                     | In situ co-precipitation of Fe <sub>3</sub> O <sub>4</sub>  | –                                | –   | Methylene blue   | 4/14 h                               | 30,13                              | Langmuir         | PSO           | 80   |
| Egg white wastes           | Iron oxides  | Hydrothermal carbonization, chemical activation and co-precipitation                                  | 20                               | –   | Crystal violet   | 4/24 h                               | 18,87                              | Langmuir         | PSO           | 81   |
| Walnut shells              | Iron oxides  | Carbothermal and microwave assisted   | –                                | 1000                                      | Methylene blue   | 7/30 min                             | 130                                | Langmuir         | –             | 82   |
| Sugarcane bagasse          | γ-Fe <sub>2</sub> O <sub>3</sub>                   | Mixing in mechanical mortar, microwave calcination  | –                                | 54,49-109,07                              | Methylene blue   | 2–10/–                               | 36,14                              | Langmuir         | PSO           | 83   |
| Rice husk                  | Fe <sub>3</sub> O <sub>4</sub>                     | Carbonization of rice husk at 400 °C, activation with ZnCl <sub>2</sub> , impregnation of iron salt   | –                                | 375,02                                    | Methylene blue   | 3/30 min                             | 17,78                              | Freundlich       | –             | 48   |
| Activated carbon           | Fe <sub>3</sub> O <sub>4</sub>                     | Ball-mill extrusion with Fe <sub>3</sub> O <sub>4</sub>   | 33,8                             | 75,4                                      | Methyl orange    | 2-11 / 24 h                          | 13,21                              | Langmuir         | –             | 74   |
| Biochar                    | Fe <sub>3</sub> O <sub>4</sub>                     | Ball-mill extrusion with Fe <sub>3</sub> O <sub>4</sub>   | 34,9                             | 90,6                                      | Methylene blue   | –/–                                  | 304,2                              | Langmuir         | PSO           | 84   |
| Carbohydrate               | Fe <sub>3</sub> O <sub>4</sub> and Fe <sup>0</sup> | Hydrothermal carbonization, activation and magnetization by thermal treatment with KOH                | 8                                | 766                                       | Methylene blue   | –/–                                  | 500,5                              | Langmuir         | PSO           | 84   |
| Corn straw                 | Fe <sup>0</sup> (nZVI)                             | NaOH activation, pyrolysis of straw at 500 °C, impregnation with iron salt                            | 38,7                             | 80,1                                      | Malachite green  | 6/–                                  | 515,77                             | Langmuir         | PSO           | 85   |
| Chicken bone               | Fe <sub>3</sub> O <sub>4</sub>                     | Pyrolysis of bones at 500 °C, potassium permanganate (KMnO <sub>4</sub> ) activation, coprecipitation | 64,7                             | 328,06                                    | Rhodamine B      | 2–10/–                               | 109,66                             | Freundlich       | PSO           | 86   |
| Pineapple crown leaf waste | Fe <sub>3</sub> O <sub>4</sub>                     | carbonization at 500 °C, KOH activation and coprecipitation method                                    | 15,0                             | 95,11 - 314,08                            | Methyl violet    | 5/–                                  | 16,76                              | Redlich-Peterson | PSO           | 49   |
| Leaf powders               | Fe <sub>3</sub> O <sub>4</sub>                     | One-step coprecipitation with ultrasonication   | 20,000,0 Oe                      | –   | Congo red        | Low pH/200 min                       | 39,7                               | Langmuir         | PSO           | 87   |
| Commercial AC              | Fe <sub>3</sub> O <sub>4</sub>                     | Solution combustion   | 4,82–13,5                        | 656-761                                   | Acid yellow      | 6,8/240min                           | 62,36                              | Langmuir         | PSO           | 72   |
| Commercial AC              | Fe <sub>3</sub> O <sub>4</sub>                     | Solution combustion   | 2,43                             | 695,8-724,4                               | Acid red         | 6,9/240min                           | 77,99                              | Langmuir         | PSO           | 73   |
|                            |  |   |                                  |   | Acid orange 7    | 2,3–9,3/225 min                      | 126,19                             | Langmuir         | PSO           |      |
|                            |  |   |                                  |   | Acid blue 129    |                                      | 83,42                              | Langmuir         | PSO           |      |

Continuation of Table 2

| 1                           | 2  | 3  | 4              | 5                 | 6                                     | 7                      | 8                                | 9  | 10                       | 11 |
|-----------------------------|--|--|----------------|-------------------|---------------------------------------|------------------------|----------------------------------|--|--------------------------|----|
| Pistachio shells            | Fe <sub>3</sub> O <sub>4</sub> /<br>C <sub>4</sub> H <sub>8</sub> SO <sub>3</sub> H/ | Steam activation and sonication  | 12.0           | –                 | Methylene blue<br>Rhodamine 6G        | 5.5/10 min             | 118.15<br>131.80<br>147.0        | Langmuir<br>Langmuir<br>Langmuir             | PSO<br>PSO<br>PSO        | 50 |
| Pomelo peels                | Fe <sub>3</sub> O <sub>4</sub>   | Hydrothermal pretreatment and pyrolysis  | –              | –                 | Pb(II)<br>Cd(II)                      | 5/360 min<br>6/360 min | 205.3<br>81.9                    | Langmuir<br>Langmuir                         | PSO<br>PSO               | 58 |
| Wheat stalk and rice husk   | Fe <sub>3</sub> O <sub>4</sub>   | Pyrolysis at 600 °C and physical comixing  | 26.1 -<br>28.6 | 13.96 -<br>22.4.6 | Pb(II)                                | 5(0.5-24 h             | 73.34 -<br>179.5                 | Langmuir                                     | PSO                      | 88 |
| Biogas residue              | Fe <sub>3</sub> O <sub>4</sub>   | Direct pyrolysis and sonochemical method   | 39.96          | 79.64             | Pb(II)<br>Cu(II)                      | 5/4 h                  | 181.82<br>75.76                  | Langmuir<br>Langmuir                         | PSO<br>PSO               | 89 |
| Palm kernel cake residue    | Fe <sub>3</sub> O <sub>4</sub>   | Magnetic BC modified with MnO by pyrolysis and impregnation with magnetic phase                            | 20.94          | 89.38             | Cd(II)<br>Cr(III)<br>Hg(II)<br>Pb(II) | 7/0,5 h                | 18.60<br>19.92<br>49.64<br>13.69 | Langmuir<br>Langmuir<br>Langmuir<br>Langmuir | PSO<br>PSO<br>PSO<br>PSO | 90 |
| Layered double hydroxides   | Fe <sub>3</sub> O <sub>4</sub>   | Impregnation with humic acid, solvothermal process, and calcination  | –              | 132.4             | Cu(II)<br>Cd(II)<br>Pb(II)            | –/–                    | 400.0<br>375.0<br>200.0          | Langmuir<br>Langmuir<br>Langmuir             | PSO<br>PSO<br>PSO        | 91 |
| Banana peels                | Fe <sub>3</sub> O <sub>4</sub>   | Magnetic BC by pyrolysis and impregnation with coprecipitation of magnetic phase                           | 39.55          | 323.2             | Cu(II)<br>Hg(II)                      | 6/–                    | 75.9<br>83.4                     | Langmuir<br>Langmuir                         | PSO<br>PSO               | 92 |
| Tea leaves                  | Fe <sub>3</sub> O <sub>4</sub> /γ-<br>Fe <sub>2</sub> O <sub>3</sub>                 | One-step pyrolysis   | 16             | 124.28            | Hg <sup>0</sup>                       | –/–                    | –                                | Langmuir                                     | PSO                      | 93 |
| Pinewood sawdust            | γ-Fe <sub>2</sub> O <sub>3</sub>   | Magnetic BC by iron salts impregnation and hydrothermal pyrolysis  | 15.58          | 43.29             | Hg(II)                                | 7/–                    | 167.2                            | Langmuir                                     | PSO                      | 94 |
| Termitte feces              | Fe <sub>3</sub> O <sub>4</sub>   | Magnetic AC by low temperature carbonization, impregnation, and high temperature for magnetic modification | 1.46           | 699               | Cr(VI)                                | 3/1 h                  | 66                               | Langmuir                                     | PSO                      | 95 |
| Peanut hull                 | γ-Fe <sub>2</sub> O <sub>3</sub>   | One step hydrothermal method with iron salt and hexamethylenediamine                                       | –              | 62.4              | Cr(VI)                                | 2/23 h                 | 142.86                           | Langmuir                                     | PSO                      | 65 |
| Blooms of alga Enteromorpha | γ-Fe <sub>2</sub> O <sub>3</sub>   | Pyrolysis at 500 °C, impregnation with iron salt   | 39.29          | –                 | Cr(VI)                                | 2-4/48 h               | 11.13                            | Langmuir                                     | PSO                      | 96 |
| Leaf powders                | Fe <sub>3</sub> O <sub>4</sub>   | One-step coprecipitation with ultra-sonication.  | 20,000.0<br>Oe | –                 | Cr(VI)                                | 2/24 h                 | 38.6                             | Langmuir                                     | PSO                      | 87 |



Magnetic biosorbents overcome the limitations of ordinary adsorbents such as high energy consumption of the separation process (e.g., sedimentation and filtration).<sup>78</sup> Moreover, magnetic biosorbents possess great potential to apply in large-scale wastewater treatment and avoid secondary pollution owing to their magnetic properties. The magnetic biosorbents loaded with pollutants can be easily removed from an aqueous solution and reused after the desorption of pollutants. Cazetta *et al.*<sup>79</sup> fabricated magnetic coconut shell biosorbents with a magnetic saturation value of 28.69 emu/g which can be conveniently removed by an external magnetic field. However, the removal of contaminants from aqueous solution by the adsorption process is affected by several conditions.<sup>75</sup> The removal efficiency of the pollutants highly depends on the characteristics of magnetic biosorbents such as specific surface area, pore structures, and surface functional groups.

Table 2 represents the results of studies on the adsorption of dyes and heavy metals by magnetic adsorbents of pollutants in the aqueous medium by magnetic iron nanocomposites derived from biomass published in scientific articles since 2018. A brief description of the sorbent, its manufacturing method, magnetization level, specific surface area, target pollutant, optimal sorption conditions, maximum adsorption capacity, as well as isotherms and kinetic models are listed in Table 2. Thus, the structure-property relationship, adsorption mechanism, and the influence of synthesis conditions are further discussed in the following sections for specific types of pollutants. It can be concluded from Table 2 that in most studies the Langmuir isotherm model and pseudo-second-order kinetic model were applied to evaluate the adsorption process.

#### 4.1. Adsorption of Dyes

The textile industry consumes a total of 700,000 tons of dyes annually.<sup>97</sup> As a result, a huge amount of dyes are discharged into wastewater, causing serious water pollution.<sup>98</sup> Dyes are highly resistant to biological and photo-degradation which makes them difficult to be removed from wastewater.<sup>99</sup> Most of the dyes block the penetration of light into the water which affects the photosynthetic activity of aquatic plants. Besides, the consumption of toxic and mutagenic molecules of dyes leads to the damage of organs of humans such as liver and kidney, as well as central nervous and reproductive systems.<sup>100</sup> Therefore, the removal of cationic and anionic dyes from wastewater is necessary before discharge into the environment.

Iron oxide nanoparticles play an important role in the preparation of magnetic biosorbents. For example, the  $\text{FeCl}_3$  solution served as a metal precursor and activating

agent during the synthesis of magnetic activated coconut shell biosorbents.<sup>79</sup> The iron oxide nanoparticles impregnated on the surface of peach gum biosorbents not only provided magnetic properties but also served as a cross-linker to bind the peach gum molecules.<sup>78</sup> The optimum ratio of iron oxide nanoparticles to biosorbents is required to achieve excellent adsorption performance. The ratio of  $\text{FeCl}_3 \cdot 6\text{H}_2\text{O}$  to coconut shells of 1:1 achieved the highest specific surface area of 372  $\text{m}^2/\text{g}$  compared to ratios of 2:1 and 3:1.<sup>79</sup> This was attributed to the excess iron oxide nanoparticles occupying the pores of the magnetic biosorbents and decreased the pore volume. Nguyen *et al.* proposed that the  $\text{Fe}_3\text{O}_4$  nanoparticles pomelo peel biosorbents ( $\text{Fe}_3\text{O}_4/\text{PPB}$ ) with  $\text{Fe}_3\text{O}_4$  to PPB ratio of 5:1 achieved a higher adsorption capacity of Reactive Red 21 (RR21) compared to  $\text{Fe}_3\text{O}_4/\text{PPB}$  with a ratio of 6:1.<sup>101</sup>

Besides, magnetic biosorbents exhibit a better adsorption performance than pristine biosorbents due to their higher specific area, pore volume, and porosity. Akpomie *et al.*<sup>102</sup> showed that novel magnetic banana (*Musa acuminata*) peels ( $\text{Fe}_3\text{O}_4/\text{BP}$ ) possessed a higher pore volume and mesoporous structure than pristine biosorbents, which allowed efficient penetration of bromophenol blue molecules through the pores.  $\text{CoFe}_2\text{O}_4$  spinel ferrite nanoparticles rice husk bio-silica ( $\text{CoFe}_2\text{O}_4/\text{RHBS}$ ) possessed 5 times higher adsorption capacity than that of the pristine RHBS due to a higher specific surface area and more available adsorption sites.<sup>103</sup> The  $\text{Fe}_3\text{O}_4/\text{PPB}$  prepared by Nguyen *et al.* demonstrated a higher adsorption capacity of RR21 (e.g., 26.82 mg/g) compared to the original PPB (e.g., 17.23 mg/g)<sup>101</sup>. This was due to the presence of  $\text{Fe}_3\text{O}_4$  intercalated between the layers of PPB and led to increasing heterogeneity, higher surface area, and porosity.

Some common adsorption mechanisms such as electrostatic interactions and hydrogen bonding occurred between magnetic biosorbents and dye molecules. The  $-\text{OH}$  and  $-\text{C}=\text{O}$  functional groups on the surface of  $\text{Fe}_3\text{O}_4/\text{BP}$  were the major adsorption sites by forming hydrogen bonding and electrostatic interactions with bromophenol blue anionic dyes.<sup>102</sup> The adsorption capacity was enhanced from 6.06 to 8.12 mg/g after the  $\text{Fe}_3\text{O}_4$  impregnation ascribed to the positive surface potential of  $\text{Fe}_3\text{O}_4/\text{BP}$ , which is indicated by the higher value of pH point of zero charges ( $\text{pH}_{\text{pzc}}$ ). For the removal of anionic sunset yellow molecules, the adsorption mechanism was mainly through hydrogen bonding and  $\pi$ - $\pi$  stacking between the magnetic biosorbents and the aromatic ring of sunset yellow dye molecules.<sup>79</sup> The oxygen atoms on the surface of magnetic biosorbents formed hydrogen bonding with the hydrogen atoms in the structure of sunset yellow.

Li *et al.*<sup>78</sup> indicated magnetic peach gum bead biosorbents (MPGB) possessed a high selectivity for the removal of cationic dyes due to the electrostatic attraction between the negatively charged surface of MPGB and the positively charged atoms (*e.g.*,  $N^+$ ) of methylene blue. Anionic dyes such as Congo red and methyl orange were less adsorbed by the MPGB due to electrostatic repulsion. Similar outcomes were observed by Vahdati-Khajeh *et al.*,<sup>81</sup> where the cationic methylene blue molecules were mainly removed through electrostatic interaction from the carboxylate functional groups on the magnetic biosorbents.

The improvement of the physicochemical properties of carbon materials through the synthesis of nanocomposites makes it possible to use them to solve the problem of treating wastewater from dyes. Many studies have shown that bio-carbon nanocomposites are effective in removing a wide range of dyes, but methylene blue is the most commonly used model dye.<sup>104-106</sup>

## 4.2. Adsorption of Heavy Metals

The toxic metal ions are released into the environment by the disposal of effluents generated in industrial activities such as smelting, paint production, and electroplating.<sup>107</sup> The negative impact of toxic element ions on the environment and humans, as well as their tendency to bioaccumulate, is of great concern.<sup>108</sup> Therefore, effective methods of toxic elements removal are extremely urgent and have attracted interest from researchers. Table 2 illustrates the adsorption conditions of some toxic elements in iron-based magnetic nanocomposites. Heavy metals are most often selected from the following list: Pb(II), Cd(II), Cu(II), Cr(III), Cr(VI), Hg(II),  $Hg^0$ . In unpolluted natural waters, the concentrations of Cd(II), Pb(II) and Zn(II) ions are 0.02-0.3  $\mu\text{g/L}$ , 1.5-6.5  $\mu\text{g/L}$  and 3-120  $\mu\text{g/L}$ , respectively. However, in places where industrial effluents are discharged into rivers, the concentration of these metals exceeds the maximum allowable concentrations by up to 10 times, resulting in their toxic effect on aquatic biota.

Carbonaceous materials, including activated carbon, carbon nanotubes and graphene oxide, have been widely studied for the adsorption of various types of heavy metals from the environment.<sup>109</sup> Kang *et al.*<sup>110</sup> evaluated the performance of magnetic activated carbon for Cd(II) and Pb(II) removal and the influence of acid treatment in the adsorption capacity. The results showed that the maximum adsorption capacities of activated carbon and activated carbon treated with nitric acid for Cd(II) removal were 6.50 and 60.4 mg/g, respectively, and 11.8 and 99.6 mg/g for Pb(II), respectively. The adsorbent capacities increased significantly with nitric acid treatment; however, there was a reduction in the

adsorption capacity when activated carbon treated with nitric acid was combined with magnetic nanoparticles, 49.8 and 86.2 mg/g for Cd(II) and Pb(II), respectively, attributed to the decrease in the active sites of activated carbon treated with nitric acid that was occupied by magnetic nanoparticles, suggesting that for activated carbon material, the magnetic nanoparticles did not contribute to the increase in the adsorption capacity of the nanocomposite, unlike other matrices.

Magnetic carbon nanocomposites with a core-shell structure were also studied. Huong *et al.*<sup>111</sup> evaluated the adsorption capacity  $Fe_3O_4@C$  for As(V). The maximum adsorption capacity obtained by the Langmuir model was 20.1 mg/g at pH 1-2. The adsorption mechanism occurred through electrostatic interactions between the functional groups of the nanocomposite, *e.g.*,  $-COOH$  and  $-OH$ , and As(V) ions, which was influenced by the structure morphology of  $Fe_3O_4@C$ . However, the quantity of adsorbed As(V) decreases with the increase in carbon content. This increase caused the encapsulation of magnetic nanoparticles, which impaired the interaction of  $-OH$  groups with arsenic ions. At low pH conditions, the number of  $H^+$  ions in the solution increased, and  $-OH$  and  $-COOH$  became positively charged  $-OH_2^+$  and  $-COOH_2^+$ , increasing the adsorption capacity of  $H_2AsO_4^-$ . The same mechanism has been reported for the adsorption of Cr(VI) in  $Fe_3O_4@C$ , whose maximum capacity of 61.7 mg/g was obtained at pH 4.0.<sup>112</sup>

Langmuir model was the one that showed the highest correlation with the experimental data and, therefore, the most used model to explain the process of adsorption of toxic elements in magnetic iron-based nanomaterials. The Langmuir isotherm model assumes monolayer coverage of adsorbates over a homogenous adsorbent surface, and after the equilibrium time, the saturation point is reached, which corresponds to the maximum of adsorption.<sup>33</sup> The experimental data of adsorption in the magnetic nanocomposites system usually follow a pseudo-second-order kinetic model, indicating that the adsorption of the toxic elements is dependent on the concentration of the adsorbed element in the nanomaterial, and element concentration in equilibrium.<sup>20</sup>

The mechanisms by which inorganic species are adsorbed onto magnetic nanocomposites may involve multiple interactions. Generally, electrostatic interaction, surface complexation, ion exchange, precipitation, and hydrogen bonding might be the primary mechanisms.<sup>32</sup> The mechanisms will depend on the chemical form of the species in solution; a speciation study is important to propose improvements in the performance of the adsorbent. Besides, the specific role of each mechanism in the toxic elements adsorptions varies depending on the adsorbent properties, such as specific surface area, functional groups, charges, and the ionic environment of

the aqueous solution.<sup>109</sup> The pH of the solution is one of the most important factors that affect not only the speciation of toxic elements but also the surface charge of the adsorbent material and the complexation behavior of functional groups.

Thermodynamic studies indicate the nature of the toxic elements adsorption. The nature of the process varied according to the matrix used in the nanocomposite. For example, the adsorption in materials based on silica,<sup>113</sup> chitosan,<sup>114,115</sup> graphene oxide,<sup>116-118</sup> and biocarbon from palm oil residue<sup>90</sup> is endothermic, that is, the amount adsorbed increased with increasing temperature. On the other hand, cellulose-based materials, the process is exothermic. The enthalpy values for most materials are less than 40 kJ/mol, so the toxic elements adsorption in magnetic nanocomposites could be considered as physical adsorption.

The type of magnetic nanoparticle used also appears to be a factor that interferes with the nature of the process. Similar to dye adsorption, the incorporation of 10 wt% iron oxides nanoparticles in orange peels improved their adsorption properties. This is explained by an increase in porosity and specific surface area.<sup>30</sup> Altaf *et al.*<sup>93</sup> utilized 0.46 mol/L of  $\text{Fe}(\text{NO}_3)_3$  solution to synthesize iron oxide nanoparticles as a catalyst to prepare magnetic waste tea leaves biosorbents (MTLB). The resultant MTLB had a great improvement in specific surface area and porous structure attributed to the release of volatile matters such as nitrogen during pyrolysis.

Moreover, the increment of oxygen content and surface functional groups in magnetic biosorbents facilitated the adsorption of heavy metal ions. Nejadshafiee *et al.*<sup>50</sup> modified  $\text{Fe}_3\text{O}_4$  nanoparticles impregnated on pistachio shells biosorbents with 1,4-butane sultone ( $\text{Fe}_3\text{O}_4/\text{PS}/\text{C}_4\text{H}_8\text{SO}_3\text{H}$ ) to increase the amount of acidic

functional groups on the magnetic biosorbents. For instance, the functional groups of sulfo ( $-\text{SO}_3\text{H}$ ) and  $-\text{OH}$  on the surface of  $\text{Fe}_3\text{O}_4/\text{PS}/\text{C}_4\text{H}_8\text{SO}_3\text{H}$  formed complex compounds with the heavy metal ions such as  $\text{Pb}(\text{II})$ ,  $\text{Cd}(\text{II})$ , and  $\text{As}(\text{III})$ . Pipiska *et al.*<sup>119</sup> indicated that the improved adsorption performance of  $\text{Co}(\text{II})$  was because of the oxygen-containing functional groups and iron oxide nanoparticles presented on the surface of magnetically functionalized *Rhynchospora squarrosa* moss biosorbents (MMB). The accumulation of  $\text{Co}(\text{II})$  was observed in the regions that are rich in iron and oxygen due to the electrostatic attractions between oxygen functional groups on magnetic biosorbents and  $\text{Co}(\text{II})$ .

The  $\text{Hg}^0$  was removed by MTLB due to the existence of oxygen-rich functional groups (*e.g.*,  $\text{C}=\text{O}$ ).<sup>93</sup> It served as an active site for  $\text{Hg}^0$  removal through the high affinity of  $\text{Hg}^0$  toward oxygen. In another study, Geng *et al.* suggested the magnetic *Forsythia suspense* leaf powder biosorbent (MFSLB) was effectively to remove  $\text{Cr}(\text{VI})$  in wastewater.<sup>87</sup> The electrostatic interactions between the MFSLB and pollutants were important since the  $\text{Cr}(\text{VI})$  ions possessed negative charges. In addition, the force of attraction was highly controlled by the pH which determined the surface charges of MFSLB.

Fig. 5. depicts the electrostatic interactions between heavy metal ions and magnetic biosorbents. To further improve the adsorption process, Nejadshafiee *et al.*<sup>50</sup> conducted the adsorption of  $\text{Pd}(\text{II})$ ,  $\text{Cd}(\text{II})$ , and  $\text{As}(\text{III})$  ions assisted by ultrasonic. It demonstrated a higher adsorption capacity of heavy metal ions compared to shaker-assisted adsorption. This was attributed to the enhanced mass transfer during adsorption and thus increased the affinity between heavy metal ions and  $\text{Fe}_3\text{O}_4/\text{PS}/\text{C}_4\text{H}_8\text{SO}_3\text{H}$ .

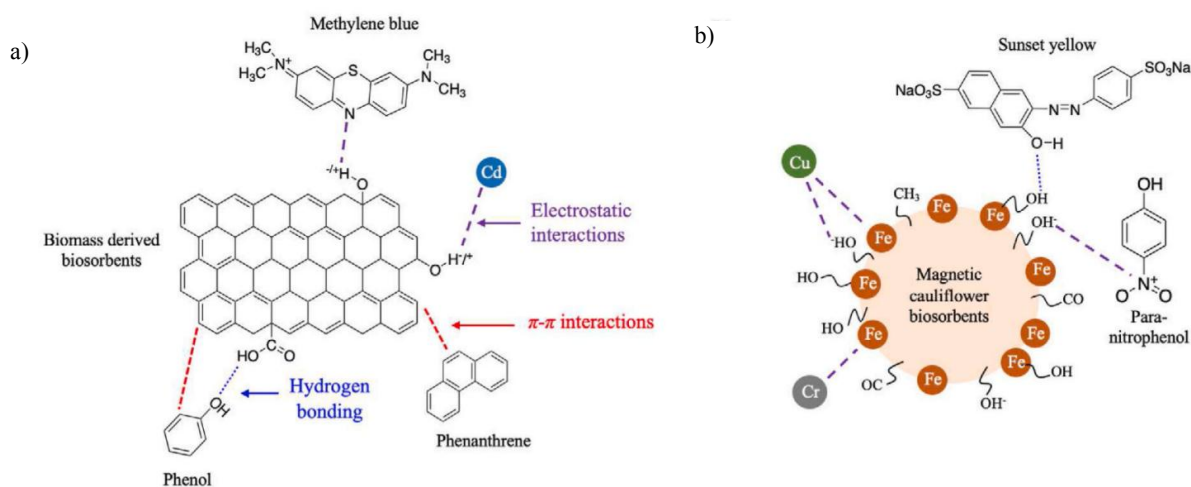


**Fig. 5.** Illustration of  $\pi$ - $\pi$  interactions, hydrogen bonding and electrostatic interactions occurred on (a) biomass derived biosorbents and (b) magnetic biosorbents.<sup>12</sup>

## 5. Conclusions

The review is devoted to the analysis of the adsorption treatment of wastewater from heavy metal ions and dyes using magnetically sensitive carbon-based nanocomposites. It has been shown that such magnetically sensitive nanocomposites have great potential for water treatment technologies due to their fast adsorption kinetics and high adsorption capacity. From the analysis of the published literature in recent years, several key points have been identified regarding the methods of synthesis and modification of carbon nanocomposites. Firstly, to synthesize economically attractive nanocomposites, it is necessary to use waste from the food industry or agricultural processing as carbon feedstock. Iron salts are the best choice as activators to promote the formation of a magnetically sensitive phase in the composite. This choice is not only economically feasible, but iron salts are also less toxic to the environment than salts of other ferromagnets. They also provide physical stability of the resulting magnetic phase in the composite and high values of specific saturation magnetization. Secondly, the synthesis of carbon nanocomposites in two or more stages contributes to a significant increase in specific surface area and specific volume. This significantly increases the adsorption capacity for various pollutants. The additional treatment also promotes surface oxidation, and the formation of additional functional groups such as –OH or –COOH, which help to increase the efficiency of the interaction between the nanocomposite surface and the pollutants.

The influence of pH of the aqueous solution, adsorbent dose, adsorption time, and temperature on the adsorption capacity of carbon nanocomposites for different dyes and heavy metal ions is summarized. It has been shown that a typical model dye is methylene blue, the adsorption of which has been studied in most of the articles analyzing dye wastewater treatment. It has been found that as the dose of adsorbent increases, the adsorption capacity decreases due to an excess of active adsorption centers. On the other hand, an increase in the initial concentration of the adsorbate in the solution and an increase in the contact time between the adsorbate and the adsorbent until equilibrium is reached contribute to an increase in the adsorption capacity. The effect of temperature on adsorption capacity depends on the nature of the adsorption process (exothermic or endothermic adsorption). It has been shown that the nature of the adsorption process is determined by the type of precursor used to synthesize the carbon matrix of the nanocomposite.

In general, such properties show the prospects for further development and improvement of magnetically sensitive nanocomposites to obtain commercial products

and their implementation in real schemes of wastewater treatment from heavy metal ions and dyes.

## Abbreviations

|       |  |
|-------|--|
| AC    | Activated carbon                             |
| BC    | Biochar                                      |
| HC    | Hydrochar                                    |
| PET   | Polyethylene terephthalate                   |
| HTC   | Hydrothermal carbonization                   |
| PAH   | Polycyclic aromatic hydrocarbon              |
| nZVI  | Nano zero-valent iron                        |
| PPB   | Pomelo peel biosorbent                       |
| BP    | Banana peels                                 |
| RHBS  | Rice husk bio-silica                         |
| RR21  | Reactive Red 21                              |
| MPGB  | Magnetic peach gum bead biosorbent           |
| MTLB  | Magnetic waste tea leaves biosorbents        |
| PS    | Pistachio shells                             |
| MMB   | Magnetically functionalized moss biosorbents |
| MFSLB | Forsythia suspense leaf powder biosorbent    |

## References

- [1] Zamora-Ledezma, C.; Negrete-Bolagay, D.; Figueroa, F.; Zamora-Ledezma, E.; Ni, M., Alexis, F.; Guerrero, V. H. Heavy metal water pollution: A fresh look about hazards, novel and conventional remediation methods. *Environ. Technol. Innov.* **2021**, *22*, 101504. <https://doi.org/10.1016/j.eti.2021.101504>
- [2] Vasiichuk, V.; Kurylets, O.; Nahurskyy, O.; Kuchera, Y.; Bukliv, R.; Kalymon, Y. Obtaining New Aluminium Water Clarification Coagulant from Spent Catalyst. *Ecol. Eng. Environ. Technol.* **2022**, *23*, 47–53. <https://doi.org/10.12912/27197050/147147>
- [3] Malovanyy, M. S.; Synelnikov, S. D.; Nagurskiy, O. A.; Soloviy, K. M.; Tymchuk, I. S. Utilization of sorted secondary PET waste-raw materials in the context of sustainable development of the modern city. In *IOP Conf. Ser.: Mater. Sci. Eng.* **2020**, *907*, 012067. <https://doi.org/10.1088/1757-899X/907/1/012067>
- [4] Garg, V. K.; Kumar, R.; Gupta, R. Removal of malachite green dye from aqueous solution by adsorption using agro-industry waste: a case study of *Prosopis cineraria*. *Dyes Pigm.* **2004**, *62*, 1–10. <https://doi.org/10.1016/j.dyepig.2003.10.016>
- [5] Verma, R.; Dwivedi, P. Heavy metal water pollution-A case study. *Recent Research in Science and Technology* **2013**, *5*, 98–99.
- [6] Razzak, S. A.; Faruque, M. O.; Alsheikh, Z.; Alsheikhmohamad, L.; Alkuroud, D.; Alfayez, A.; Hossain, S.; Hossain, M.M. A comprehensive review on conventional and biological-driven heavy metals removal from industrial wastewater. *Environ. Adv.* **2022**, *7*, 100168. <https://doi.org/10.1016/j.envadv.2022.100168>
- [7] Moosavi, S.; Lai, C. W.; Gan, S.; Zamiri, G.; Akbarzadeh Pivezhani, O.; Johan, M. R. Application of efficient magnetic particles and activated carbon for dye removal from wastewater. *ACS Omega* **2020**, *5*, 20684–20697. <https://doi.org/10.1021/acsomega.0c01905>
- [8] Nahurskiy, O.; Krylova, H.; Vasiichuk, V.; Kachan, S.; Nahursky, A.; Paraniak, N.; Sabadash, V.; Malovanyy, M. Utilization of Household Plastic Waste in Technologies with Final

- Biodegradation. *Ecol. Eng. Environ. Technol.* **2022**, *23*, 94–100. <https://doi.org/10.12912/27197050/150234>
- [9] Shrestha, R.; Ban, S.; Devkota, S.; Sharma, S.; Joshi, R.; Tiwari, A. P.; Kim, H. Y.; Joshi, M. K. Technological trends in heavy metals removal from industrial wastewater: A review. *J. Environ. Chem. Eng.* **2021**, *9*, 105688. <https://doi.org/10.1016/j.jece.2021.105688>
- [10] Nagurskyi, O.; Krylova, H.; Vasiichuk, V.; Kachan, S.; Dziurakh, Y.; Nahurskyi, A.; Paraniak, N. Safety Usage of Encapsulated Mineral Fertilizers Based on Polymeric Waste. *Ecol. Eng. Environ. Technol.* **2022**, *23*, 156–161. <https://doi.org/10.12912/27197050/143139>
- [11] Qasem, N. A.; Mohammed, R. H.; Lawal, D. U. Removal of heavy metal ions from wastewater: A comprehensive and critical review. *npj Clean Water.* **2021**, *4*, 36. <https://doi.org/10.1038/s41545-021-00127-0>
- [12] Tee, G. T.; Gok, X. Y.; Yong, W. F. Adsorption of pollutants in wastewater via biosorbents, nanoparticles and magnetic biosorbents: A review. *Environ. Res.* **2022**, *212*, 113248. <https://doi.org/10.1016/j.envres.2022.113248>
- [13] Sharma, A.; Mangla, D.; Chaudhry, S. A. Recent advances in magnetic composites as adsorbents for wastewater remediation. *J. Environ. Manage.* **2022**, *306*, 114483. <https://doi.org/10.1016/j.jenvman.2022.114483>
- [14] Bordun, I.; Vasylynych, T.; Malovanyy, M.; Sakalova, H.; Liubchak, L.; Luchyt, L. Study of adsorption of differently charged dyes by carbon adsorbents. *Desalin. Water Treat.* **2023**, *288*, 151–158. <https://doi.org/10.5004/dwt.2023.29332>
- [15] Santhosh, C.; Daneshvar, E.; Tripathi, K. M.; Baltrėnas, P.; Kim, T.; Baltrėnaitė, E.; Bhatnagar, A. Synthesis and characterization of magnetic biochar adsorbents for the removal of Cr (VI) and Acid orange 7 dye from aqueous solution. *Environ. Sci. Pollut. Res.* **2020**, *27*, 32874–32887. <https://doi.org/10.1007/s11356-020-09275-1>
- [16] Sivashankar, R.; Sathya, A. B.; Vasantharaj, K.; Sivasubramanian, V. Magnetic composite an environmental super adsorbent for dye sequestration—A review. *Environ. Nanotechnol. Monit. Manage.* **2014**, *1*, 36–49. <https://doi.org/10.1016/j.enmm.2014.06.001>
- [17] Soares, S. F.; Fernandes, T.; Trindade, T.; Daniel-da-Silva, A. L. Recent advances on magnetic biosorbents and their applications for water treatment. *Environ. Chem. Lett.* **2020**, *18*, 151–164. <https://doi.org/10.1007/s10311-019-00931-8>
- [18] Madhura, L.; Singh, S.; Kanchi, S.; Sabela, M.; Bisetty, K.; Inamuddin. Nanotechnology-based water quality management for wastewater treatment. *Environ. Chem. Lett.* **2019**, *17*, 65–121. <https://doi.org/10.1007/s10311-018-0778-8>
- [19] Sousa, F. L.; Daniel-da-Silva, A. L.; Silva, N. J. O.; Trindade, T. Bionanocomposites for magnetic removal of water pollutants. In *Eco-friendly polymer nanocomposites: chemistry and applications*, Vol 74; Springer, 2015; pp 279–310. [https://doi.org/10.1007/978-81-322-2473-0\\_9](https://doi.org/10.1007/978-81-322-2473-0_9)
- [20] Mehta, D.; Mazumdar, S.; Singh, S. K. Magnetic adsorbents for the treatment of water/wastewater—a review. *J. Water Process Eng.* **2015**, *7*, 244–265. <https://doi.org/10.1016/j.jwpe.2015.07.001>
- [21] Simeonidis, K.; Mourdikoudis, S.; Kaprara, E.; Mitrakas, M.; Polavarapu, L. Inorganic engineered nanoparticles in drinking water treatment: a critical review. *Environ. Sci. Water Res. Technol.* **2016**, *2*, 43–70. <https://doi.org/10.1039/C5EW00152H>
- [22] Adeleye, A. S.; Conway, J. R.; Garner, K.; Huang, Y.; Su, Y.; Keller, A. A. Engineered nanomaterials for water treatment and remediation: Costs, benefits, and applicability. *Chem. Eng. J.* **2016**, *286*, 640–662. <https://doi.org/10.1016/j.cej.2015.10.105>
- [23] Reddy, D. H. K.; Yun, Y. S. Spinel ferrite magnetic adsorbents: alternative future materials for water purification? *Coord. Chem. Rev.* **2016**, *315*, 90–111. <https://doi.org/10.1016/j.ccr.2016.01.012>
- [24] Behrens, S.; Appel, I. Magnetic nanocomposites. *Curr. Opin. Biotechnol.* **2016**, *39*, 89–96. <https://doi.org/10.1016/J.COPBI.2016.02.005>
- [25] Abdullah, N. H.; Shamel, K.; Abdullah, E. C.; Abdullah, L. C. Solid matrices for fabrication of magnetic iron oxide nanocomposites: synthesis, properties, and application for the adsorption of heavy metal ions and dyes. *Composites, Part B* **2019**, *162*, 538–568. <https://doi.org/10.1016/j.compositesb.2018.12.075>
- [26] Khan, S. T.; Malik, A. Engineered nanomaterials for water decontamination and purification: From lab to products. *J. Hazard. Mater.* **2019**, *363*, 295–308. <https://doi.org/10.1016/j.jhazmat.2018.09.091>
- [27] Siddiqui, M. T. H.; Nizamuddin, S.; Baloch, H. A.; Mubarak, N. M.; Al-Ali, M.; Mazari, S. A.; Bhutto, A. W.; Abro, A.; Srinivasan, M.; Griffin, G. Fabrication of advanced magnetic carbon nano-materials and their potential applications: a review. *J. Environ. Chem. Eng.* **2019**, *7*, 102812. <https://doi.org/10.1016/j.jece.2018.102812>
- [28] Rudakov, G. A.; Tsiberkin, K. B.; Ponomarev, R. S.; Henner, V. K.; Ziolkowska, D. A.; Jasinski, J. B.; Sumanasekera, G. Magnetic properties of transition metal nanoparticles enclosed in carbon nanocages. *J. Magn. Magn. Mater.* **2019**, *472*, 34–39. <https://doi.org/10.1016/j.jmmm.2018.10.016>
- [29] Bordun, I.; Chwastek, K.; Calus, D.; Chabecki, P.; Ivashchyn, F.; Kohut, Z.; Borysiuk, A.; Kulyk, Y. Comparison of structure and magnetic properties of Ni/C composites synthesized from wheat straw by different methods. *Appl. Sci.* **2021**, *11*, 10031. <https://doi.org/10.3390/app112110031>
- [30] Meng, F.; Yang, B.; Wang, B.; Duan, S.; Chen, Z.; Ma, W. Novel dendrimer like magnetic biosorbent based on modified orange peel waste: Adsorption–reduction behavior of arsenic. *ACS Sustainable Chem. Eng.* **2017**, *5*, 9692–9700. <https://doi.org/10.1021/acsschemeng.7b01273>
- [31] Zhang, Y.; Wu, B.; Xu, H.; Liu, H.; Wang, M.; He, Y.; Pan, B. Nanomaterials-enabled water and wastewater treatment. *NanoImpact* **2016**, *3*, 22–39. <https://doi.org/10.1016/j.impact.2016.09.004>
- [32] Wang, T.; Ai, S.; Zhou, Y.; Luo, Z.; Dai, C.; Yang, Y.; Zhang, J.; Huang, H.; Luo, S.; Luo, L. Adsorption of agricultural wastewater contaminated with antibiotics, pesticides and toxic metals by functionalized magnetic nanoparticles. *J. Environ. Chem. Eng.* **2018**, *6*, 6468–6478. <https://doi.org/10.1016/j.jece.2018.10.014>
- [33] Chen, L.; Zhou, C. H.; Fiore, S.; Tong, D. S.; Zhang, H.; Li, C. S.; Ji, S. F.; Yu, W. H. Functional magnetic nanoparticle/clay mineral nanocomposites: preparation, magnetism and versatile applications. *Appl. Clay Sci.* **2016**, *127*, 143–163. <https://doi.org/10.1016/j.clay.2016.04.009>
- [34] Baghdadi, M.; Ghaffari, E.; & Aminzadeh, B. Removal of carbamazepine from municipal wastewater effluent using optimally synthesized magnetic activated carbon: adsorption and sedimentation kinetic studies. *J. Environ. Chem. Eng.* **2016**, *4*, 3309–3321. <https://doi.org/10.1016/j.jece.2016.06.034>
- [35] Donia, A. M.; Atia, A. A.; Abouzayed, F. I. Preparation and characterization of nano-magnetic cellulose with fast kinetic properties towards the adsorption of some metal ions. *Chem. Eng. J.* **2012**, *191*, 22–30. <https://doi.org/10.1016/j.cej.2011.08.034>

- [36] Guo, X.; Du, B.; Wei, Q.; Yang, J.; Hu, L.; Yan, L.; Xu, W. Synthesis of amino functionalized magnetic graphenes composite material and its application to remove Cr (VI), Pb (II), Hg (II), Cd (II) and Ni (II) from contaminated water. *J. Hazard. Mater.* **2014**, *278*, 211–220. <https://doi.org/10.1016/j.jhazmat.2014.05.075>
- [37] Zhou, L.; Ji, L.; Ma, P. C.; Shao, Y.; Zhang, H.; Gao, W.; Li, Y. Development of carbon nanotubes/CoFe<sub>2</sub>O<sub>4</sub> magnetic hybrid material for removal of tetrabromobisphenol A and Pb (II). *J. Hazard. Mater.* **2014**, *265*, 104–114. <https://doi.org/10.1016/j.jhazmat.2013.11.058>
- [38] Masoumi, A.; Hemmati, K.; Ghaemy, M. Recognition and selective adsorption of pesticides by superparamagnetic molecularly imprinted polymer nanospheres. *RSC adv.* **2016**, *6*, 49401–49410. <https://doi.org/10.1039/c6ra05873f>
- [39] Kheshti, Z.; Hassanajili, S. Novel multifunctional mesoporous microsphere with high surface area for removal of zinc ion from aqueous solution: preparation and characterization. *J. Inorg. Organomet. Polym. Mater.* **2017**, *27*, 1613–1626. <https://doi.org/10.1007/s10904-017-0621-x>
- [40] Li, R.; An, Q. D.; Mao, B. Q.; Xiao, Z. Y.; Zhai, S. R.; Shi, Z. PDA-mediated green synthesis of amino-modified, multifunctional magnetic hollow composites for Cr(VI) efficient removal. *J. Taiwan Inst. Chem. Eng.* **2017**, *80*, 596–606. <https://doi.org/10.1016/j.jtice.2017.08.036>
- [41] Langeroudi, M. P.; Binaeian, E. Tannin-APTES modified Fe<sub>3</sub>O<sub>4</sub> nanoparticles as a carrier of Methotrexate drug: kinetic, isotherm and thermodynamic studies. *Mater. Chem. Phys.* **2018**, *218*, 210–217. <https://doi.org/10.1016/j.matchemphys.2018.07.044>
- [42] Marcelo, L. R.; de Gois, J. S.; da Silva, A. A.; Cesar, D. V. Synthesis of iron-based magnetic nanocomposites and applications in adsorption processes for water treatment: a review. *Environ. Chem. Lett.* **2021**, *19*, 1229–1274. <https://doi.org/10.1007/s10311-020-01134-2>
- [43] Lu, F.; Astruc, D. Nanomaterials for removal of toxic elements from water. *Coord. Chem. Rev.* **2018**, *356*, 147–164. <https://doi.org/10.1016/j.ccr.2017.11.003>
- [44] Nadar, S. S.; Varadan, N.; Suresh, S.; Rao, P.; Ahirrao, D. J.; Adsare, S. Recent progress in nanostructured magnetic framework composites (MFCs): synthesis and applications. *J. Taiwan Inst. Chem. Eng.* **2018**, *91*, 653–677. <https://doi.org/10.1016/j.jtice.2018.06.029>
- [45] Li, N.; Jiang, H. L.; Wang, X.; Wang, X.; Xu, G.; Zhang, B.; Wang, L.; Zhao, R. S.; Lin, J. M. Recent advances in graphene-based magnetic composites for magnetic solid-phase extraction. *TrAC, Trends Anal. Chem.* **2018**, *102*, 60–74. <https://doi.org/10.1016/j.trac.2018.01.009>
- [46] Soloviy, C.; Malovanyy, M.; Bordun, I.; Ivashchyshyn, F.; Borysiuk, A.; Kulyk, Y. Structural, magnetic and adsorption characteristics of magnetically susceptible carbon sorbents based on natural raw materials. *J. Water Land Dev.* **2020**, *47*, 160–168. <https://doi.org/10.24425/jwld.2020.135043>
- [47] Reynel-Ávila, H. E.; Camacho-Aguilar, K. I.; Bonilla-Petriciolet, A.; Mendoza-Castillo, D. I.; González-Ponce, H. A.; Trejo-Valencia, R. Engineered magnetic carbon-based adsorbents for the removal of water priority pollutants: an overview. *Adsorpt. Sci. Technol.* **2021**, 1–41. <https://doi.org/10.1155/2021/9917444>
- [48] Azam, K.; Raza, R.; Shezad, N.; Shabir, M.; Yang, W.; Ahmad, N.; Shafiq, I.; Akhter, P.; Razaq, A.; Hussain, M. Development of recoverable magnetic mesoporous carbon adsorbent for removal of methyl blue and methyl orange from wastewater. *J. Environ. Chem. Eng.* **2020**, *8*, 104220. <https://doi.org/10.1016/j.jece.2020.104220>
- [49] Astuti, W.; Sulistyaningsih, T.; Kusumastuti, E.; Thomas, G. Y. R. S.; Kusnadi, R. Y. Thermal conversion of pineapple crown leaf waste to magnetized activated carbon for dye removal. *Bioresour. Technol.* **2019**, *287*, 121426. <https://doi.org/10.1016/j.biortech.2019.121426>
- [50] Nejadshafiee, V.; Islami, M. R. Adsorption capacity of heavy metal ions using sultone-modified magnetic activated carbon as a bio-adsorbent. *Mater. Sci. Eng., C.* **2019**, *101*, 42–52. <https://doi.org/10.1016/j.msec.2019.03.081>
- [51] Chen, Y.; Liu, Y.; Li, Y.; Chen, Y.; Wu, Y.; Li, H.; Wang, S.; Peng, Z.; Xu, R.; Zeng, Z. Novel magnetic pomelo peel biochar for enhancing Pb (II) and Cu (II) adsorption: performance and mechanism. *Water Air Soil Pollut.* **2020**, *231*, 404. <https://doi.org/10.1007/s11270-020-04788-4>
- [52] Bordun, I.; Szymczykiwicz, E. Synthesis and Electrochemical Properties of Fe<sub>3</sub>O<sub>4</sub>/C Nanocomposites for Symmetric Supercapacitors. *Appl. Sci.* **2024**, *14*, 677. <https://doi.org/10.3390/app14020677>
- [53] Acosta, R.; Nabarlaz, D.; Sánchez-Sánchez, A.; Jagiello, J.; Gadonneix, P.; Celzard, A.; Fierro, V. Adsorption of Bisphenol A on KOH-activated tyre pyrolysis char. *J. Environ. Chem. Eng.* **2018**, *6*, 823–833. <https://doi.org/10.1016/j.jece.2018.01.002>
- [54] Zúñiga-Muro, N. M.; Bonilla-Petriciolet, A.; Mendoza-Castillo, D. I.; Duran-Valle, C. J.; Silvestre-Albero, J.; Reynel-Ávila, H. E.; Tapia-Picazo, J. C. Recycling of Tetra pak wastes via pyrolysis: Characterization of solid products and application of the resulting char in the adsorption of mercury from water. *J. Cleaner Prod.* **2021**, *291*, 125219. <https://doi.org/10.1016/j.jclepro.2020.125219>
- [55] Singh, E.; Kumar, A.; Khapre, A.; Saikia, P.; Shukla, S. K.; Kumar, S. Efficient removal of arsenic using plastic waste char: Prevailing mechanism and sorption performance. *J. Water Process Eng.* **2020**, *33*, 101095. <https://doi.org/10.1016/j.jwpe.2019.101095>
- [56] Korchak, B.; Grynshyn, O.; Chervinskyy, T.; Nagurskyy, A.; Stadnik, V. Integrated Regeneration Method for Used Mineral Motor Oils. *Chem. Chem. Technol.* **2021**, *15*, 239–246. <https://doi.org/10.23939/chct15.02.239>
- [57] Korchak, B.; Grynshyn, O.; Chervinskyy, T.; Shapoval, P.; Nagurskyy, A. Thermooxidative Regeneration of used Mineral Motor Oils. *Chem. Chem. Technol.* **2020**, *14*, 129–134. <https://doi.org/10.23939/chct14.01.129>
- [58] Chen, Y.; Zhu, Y.; Wang, Z.; Li, Y.; Wang, L.; Ding, L.; Gao, X.; Ma, Y.; Guo, Y. Application studies of activated carbon derived from rice husks produced by chemical-thermal process—A review. *Adv. Colloid Interface Sci.* **2011**, *163*, 39–52. <https://doi.org/10.1016/j.cis.2011.01.006>
- [59] Noor, N. M.; Othman, R.; Mubarak, N. M.; Abdullah, E. C. Agricultural biomass-derived magnetic adsorbents: Preparation and application for heavy metals removal. *J. Taiwan Inst. Chem. Eng.* **2017**, *78*, 168–177. <https://doi.org/10.1016/j.jtice.2017.05.023>
- [60] Fakkaw, K.; Koottatep, T.; Polprasert, C. Effects of hydrolysis and carbonization reactions on hydrochar production. *Bioresour. Technol.* **2015**, *192*, 328–334. <https://doi.org/10.1016/j.biortech.2015.05.091>
- [61] Takaya, C. A.; Parmar, K. R.; Fletcher, L. A.; Ross, A. B. Biomass-derived carbonaceous adsorbents for trapping ammonia. *Agriculture* **2019**, *9*, 16. <https://doi.org/10.3390/agriculture9010016>
- [62] Azzaz, A. A.; Khiari, B.; Jellali, S.; Ghimbeu, C. M.; Jeguirim, M. Hydrochars production, characterization and application for wastewater treatment: A review. *Renewable Resour. J.* **2020**, *127*, 109882. <https://doi.org/10.1016/j.rser.2020.109882>

- [63] Yu, X.; Liu, S.; Lin, G.; Yang, Y.; Zhang, S.; Zhao, H.; Zheng, C.; Gao, X. KOH-activated hydrochar with engineered porosity as sustainable adsorbent for volatile organic compounds. *Colloids Surf., A*. **2020**, *588*, 124372. <https://doi.org/10.1016/j.colsurfa.2019.124372>
- [64] Abdullah, R. F.; Rashid, U.; Ibrahim, M. L.; Hazmi, B.; Alharthi, F. A.; Nehdi, I. A. Bifunctional nano-catalyst produced from palm kernel shell via hydrothermal-assisted carbonization for biodiesel production from waste cooking oil. *Renewable Sustainable Energy Rev.* **2021**, *137*, 110638. <https://doi.org/10.1016/j.rser.2020.110638>
- [65] Cai, W.; Wei, J.; Li, Z.; Liu, Y.; Zhou, J.; Han, B. Preparation of amino-functionalized magnetic biochar with excellent adsorption performance for Cr (VI) by a mild one-step hydrothermal method from peanut hull. *Colloids Surf. A*. **2019**, *563*, 102–111. <https://doi.org/10.1016/j.colsurfa.2018.11.062>
- [66] Kazak, O.; Eker, Y. R.; Bingol, H.; Tor, A. Novel preparation of activated carbon by cold oxygen plasma treatment combined with pyrolysis. *Chem. Eng. J.* **2017**, *325*, 564–575. <https://doi.org/10.1016/j.cej.2017.05.107>
- [67] Guo, J.; Lua, A. C. Preparation of activated carbons from oil-palm-stone chars by microwave-induced carbon dioxide activation. *Carbon*. **2000**, *38*, 1985–1993. [https://doi.org/10.1016/S0008-6223\(00\)00046-4](https://doi.org/10.1016/S0008-6223(00)00046-4)
- [68] Liu, W. J.; Tian, K.; He, Y. R.; Jiang, H.; Yu, H. Q. High-yield harvest of nanofibers/mesoporous carbon composite by pyrolysis of waste biomass and its application for high durability electrochemical energy storage. *Environ. Sci. Technol.* **2014**, *48*, 13951–13959. <https://doi.org/10.1021/es504184c>
- [69] Zhu, X.; Qian, F.; Liu, Y.; Matera, D.; Wu, G.; Zhang, S.; Chen, J. Controllable synthesis of magnetic carbon composites with high porosity and strong acid resistance from hydrochar for efficient removal of organic pollutants: an overlooked influence. *Carbon*. **2016**, *99*, 338–347. <https://doi.org/10.1016/j.carbon.2015.12.044>
- [70] Theydan, S. K.; Ahmed, M. J. Adsorption of methylene blue onto biomass-based activated carbon by FeCl<sub>3</sub> activation: Equilibrium, kinetics, and thermodynamic studies. *J. Anal. Appl. Pyrolysis*. **2012**, *97*, 116–122. <https://doi.org/10.1016/j.jaap.2012.05.008>
- [71] Oliveira, L. C.; Pereira, E.; Guimaraes, I. R.; Vallone, A.; Pereira, M.; Mesquita, J. P.; Sapag, K. Preparation of activated carbons from coffee husks utilizing FeCl<sub>3</sub> and ZnCl<sub>2</sub> as activating agents. *J. Hazard. Mater.* **2009**, *165*, 87–94. <https://doi.org/10.1016/j.jhazmat.2008.09.064>
- [72] Nistor, M. A.; Muntean, S. G.; Ianoş, R.; Racoviceanu, R.; Ianaşi, C.; Cseh, L. Adsorption of anionic dyes from wastewater onto magnetic nanocomposite powders synthesized by combustion method. *Appl. Sci.* **2021**, *11*, 9236. <https://doi.org/10.3390/app11199236>
- [73] Ianoş, R.; Păcurariu, C.; Muntean, S. G.; Muntean, E.; Nistor, M. A.; Nižňanský, D. Combustion synthesis of iron oxide/carbon nanocomposites, efficient adsorbents for anionic and cationic dyes removal from wastewaters. *J. Alloys Compd.* **2018**, *741*, 1235–1246. <https://doi.org/10.1016/j.jallcom.2018.01.240>
- [74] Li, Y.; Zimmerman, A. R.; He, F.; Chen, J.; Han, L.; Chen, H.; Han, L.; Chen, H.; Hu, X.; Gao, B. Solvent-free synthesis of magnetic biochar and activated carbon through ball-mill extrusion with Fe<sub>3</sub>O<sub>4</sub> nanoparticles for enhancing adsorption of methylene blue. *Sci. Total Environ.* **2020**, *722*, 137972. <https://doi.org/10.1016/j.scitotenv.2020.137972>
- [75] Tang, S. C.; Lo, I. M. Magnetic nanoparticles: essential factors for sustainable environmental applications. *Water Res.* **2013**, *47*, 2613–2632. <https://doi.org/10.1016/j.watres.2013.02.039>
- [76] Zhang, X.; Lv, L.; Qin, Y.; Xu, M.; Jia, X.; Chen, Z. Removal of aqueous Cr (VI) by a magnetic biochar derived from Melia azedarach wood. *Bioresour. Technol.* **2018**, *256*, 1–10. <https://doi.org/10.1016/j.biortech.2018.01.145>
- [77] Dong, C. D.; Chen, C. W.; Hung, C. M. Synthesis of magnetic biochar from bamboo biomass to activate persulfate for the removal of polycyclic aromatic hydrocarbons in marine sediments. *Bioresour. Technol.* **2017**, *245*, 188–195. <https://doi.org/10.1016/j.biortech.2017.08.204>
- [78] Li, C.; Wang, X.; Meng, D.; Zhou, L. Facile synthesis of low-cost magnetic biosorbent from peach gum polysaccharide for selective and efficient removal of cationic dyes. *Int. J. Biol. Macromol.* **2018**, *107*, 1871–1878. <https://doi.org/10.1016/j.ijbiomac.2017.10.058>
- [79] Cazetta, A. L.; Pezoti, O.; Bedin, K. C.; Silva, T. L.; Paesano Junior, A.; Asefa, T.; Almeida, V. C. Magnetic activated carbon derived from biomass waste by concurrent synthesis: efficient adsorbent for toxic dyes. *ACS Sustainable Chem. Eng.* **2016**, *4*, 1058–1068. <https://doi.org/10.1021/acssuschemeng.5b01141>
- [80] Adeogun, A. I.; Akande, J. A.; Idowu, M. A.; Kareem, S. O. Magnetic tuned sorghum husk biosorbent for effective removal of cationic dyes from aqueous solution: isotherm, kinetics, thermodynamics and optimization studies. *Appl. Water Sci.* **2019**, *9*, 160. <https://doi.org/10.1007/s13201-019-1037-2>
- [81] Vahdati-Khajeh, S.; Zirak, M.; Tejrak, R. Z.; Fathi, A.; Lamei, K.; Eftekhari-Sis, B. Biocompatible magnetic N-rich activated carbon from egg white biomass and sucrose: Preparation, characterization and investigation of dye adsorption capacity from aqueous solution. *Surf. Interfaces*. **2019**, *15*, 157–165. <https://doi.org/10.1016/j.surfin.2019.03.003>
- [82] Salem, S.; Teimouri, Z.; Salem, A. Fabrication of magnetic activated carbon by carbothermal functionalization of agriculture waste via microwave-assisted technique for cationic dye adsorption. *Adv. Powder Technol.* **2020**, *31*, 4301–4309. <https://doi.org/10.1016/j.apt.2020.09.007>
- [83] Jiang, W.; Zhang, L.; Guo, X.; Yang, M.; Lu, Y.; Wang, Y.; Zheng, Y.; Wei, G. Adsorption of cationic dye from water using an iron oxide/activated carbon magnetic composites prepared from sugarcane bagasse by microwave method. *Environ. Technol.* **2019**, *42*, 337–350. <https://doi.org/10.1080/09593330.2019.1627425>
- [84] Vieira, L. H. S.; Sabino, C. M. S.; Júnior, F. H. S.; Rocha, J. S.; Castro, M. O.; Alencar, R. S.; da Costa, I. S.; Viana, B. C.; de Paula, A. J.; Ferreira, O. P. et al. Strategic design of magnetic carbonaceous nanocomposites and its application as multifunctional adsorbent. *Carbon* **2020**, *161*, 758–771. <https://doi.org/10.1016/j.carbon.2020.01.089>
- [85] Eltaweil, A. S.; Mohamed, H. A.; Abd El-Monaem, E. M.; El-Subruiti, G. M. Mesoporous magnetic biochar composite for enhanced adsorption of malachite green dye: Characterization, adsorption kinetics, thermodynamics and isotherms. *Adv. Powder Technol.* **2020**, *31*, 1253–1263. <https://doi.org/10.1016/j.apt.2020.01.005>
- [86] Oladipo, A. A.; Ifebajo, A. O. Highly efficient magnetic chicken bone biochar for removal of tetracycline and fluorescent dye from wastewater: two-stage adsorbent analysis. *J. Environ. Manage.* **2018**, *209*, 9–16. <https://doi.org/10.1016/j.jenvman.2017.12.030>

- [87] Geng, J.; Chang, J. Synthesis of magnetic *Forsythia suspensa* leaf powders for removal of metal ions and dyes from wastewater. *J. Environ. Chem. Eng.* **2020**, *8*, 104224. <https://doi.org/10.1016/j.jece.2020.104224>
- [88] Li, Y.; Zhang, X.; Zhang, P.; Liu, X.; Han, L. Facile fabrication of magnetic bio-derived chars by co-mixing with Fe<sub>3</sub>O<sub>4</sub> nanoparticles for effective Pb<sup>2+</sup> adsorption: properties and mechanism. *J. Cleaner Prod.* **2020**, *262*, 121350. <https://doi.org/10.1016/j.jclepro.2020.121350>
- [89] Pan, J.; Gao, B.; Wang, S.; Guo, K.; Xu, X.; Yue, Q. Waste-to-resources: Green preparation of magnetic biogas residues-based biochar for effective heavy metal removals. *Sci. Total Environ.* **2020**, *737*, 140283. <https://doi.org/10.1016/j.scitotenv.2020.140283>
- [90] Manechakr, P.; Mongkollertlop, S. Investigation on adsorption behaviors of heavy metal ions (Cd<sup>2+</sup>, Cr<sup>3+</sup>, Hg<sup>2+</sup> and Pb<sup>2+</sup>) through low-cost/active manganese dioxide-modified magnetic biochar derived from palm kernel cake residue. *J. Environ. Chem. Eng.* **2020**, *8*, 104467. <https://doi.org/10.1016/j.jece.2020.104467>
- [91] Hou, T.; Yan, L.; Li, J.; Yang, Y.; Shan, L.; Meng, X.; Li, X.; Zhao, Y. Adsorption performance and mechanistic study of heavy metals by facile synthesized magnetic layered double oxide/carbon composite from spent adsorbent. *Chem. Eng. J.* **2020**, *384*, 123331. <https://doi.org/10.1016/j.cej.2019.123331>
- [92] Oladipo, A. A.; Ahaka, E. O.; Gazi, M. High adsorptive potential of calcined magnetic biochar derived from banana peels for Cu<sup>2+</sup>, Hg<sup>2+</sup>, and Zn<sup>2+</sup> ions removal in single and ternary systems. *Environ. Sci. Pollut. Res.* **2019**, *26*, 31887–31899. <https://doi.org/10.1007/s11356-019-06321-5>
- [93] Altaf, A. R.; Teng, H.; Zheng, M.; Ashraf, I.; Arsalan, M.; Rehman, A. U.; Gang, I.; Pengjie, W.; Yongqiang, R.; Xiaoyu, L. One-step synthesis of renewable magnetic tea-biochar derived from waste tea leaves for the removal of Hg<sup>0</sup> from coal-syngas. *J. Environ. Chem. Eng.* **2021**, *9*, 105313. <https://doi.org/10.1016/j.jece.2021.105313>
- [94] Wang, H.; Liu, Y.; Iftikhar, J.; Shi, L.; Khan, A.; Chen, Z.; Chen, Z. Towards a better understanding on mercury adsorption by magnetic bio-adsorbents with  $\gamma$ -Fe<sub>2</sub>O<sub>3</sub> from pinewood sawdust derived hydrochar: Influence of atmosphere in heat treatment. *Bioresour. Technol.* **2018**, *256*, 269–276. <https://doi.org/10.1016/j.biortech.2018.02.019>
- [95] Demarchi, C. A.; Michel, B. S.; Nedelko, N.; Ślowska-Waniewska, A.; Dłużewski, P.; Kaleta, A.; Minikayev, R.; Strachowski, T.; Lipińska, L.; Dal Magro, J.; et al. Preparation, characterization, and application of magnetic activated carbon from termite feces for the adsorption of Cr (VI) from aqueous solutions. *Powder Technol.* **2019**, *354*, 432–441. <https://doi.org/10.1016/j.powtec.2019.06.020>
- [96] Qiao, K.; Tian, W.; Bai, J.; Zhao, J.; Du, Z.; Song, T.; Chu, M.; Wang, L.; Xie, W. Synthesis of floatable magnetic iron/biochar beads for the removal of chromium from aqueous solutions. *Environ. Technol. Innovation.* **2020**, *19*, 100907. <https://doi.org/10.1016/j.eti.2020.100907>
- [97] Aguayo-Villarreal, I. A.; Cortes-Arriagada, D.; Rojas-Mayorga, C. K.; Pineda-Urbina, K.; Muñoz-Valencia, R.; Gonzalez, J. Importance of the interaction adsorbent-adsorbate in the dyes adsorption process and DFT modeling. *J. Mol. Struct.* **2020**, *1203*, 127398. <https://doi.org/10.1016/j.molstruc.2019.127398>
- [98] Ali, I.; Peng, C.; Khan, Z. M.; Sultan, M.; Naz, I. Green synthesis of phytogenic magnetic nanoparticles and their applications in the adsorptive removal of crystal violet from aqueous solution. *Arabian J. Sci. Eng.* **2018**, *43*, 6245–6259. <https://doi.org/10.1007/s13369-018-3441-6>
- [99] El-Gamal, S. M. A.; Amin, M. S.; Ahmed, M. A. Removal of methyl orange and bromophenol blue dyes from aqueous solution using Sorrel's cement nanoparticles. *J. Environ. Chem. Eng.* **2015**, *3*, 1702–1712. <https://doi.org/10.1016/j.jece.2015.06.022>
- [100] Mtshatsheni, K. N. G.; Ofomaja, A. E.; Naidoo, E. B. Synthesis and optimization of reaction variables in the preparation of pinemagnetite composite for removal of methylene blue dye. *S. Afr. J. Chem. Eng.* **2019**, *29*, 33–41. <https://doi.org/10.1016/j.sajce.2019.05.002>
- [101] Nguyen, V. H.; Van, H. T.; Nguyen, V. Q.; Dam, X. V.; Hoang, L. P.; Ha, L. T. Magnetic Fe<sub>3</sub>O<sub>4</sub> nanoparticle biochar derived from pomelo peel for reactive Red 21 adsorption from aqueous solution. *J. Chem.* **2020**, 3080612. <https://doi.org/10.1155/2020/3080612>
- [102] Akpomie, K. G.; Conradie, J. Efficient synthesis of magnetic nanoparticle-Musa acuminata peel composite for the adsorption of anionic dye. *Arabian J. Chem.* **2020**, *13*, 7115–7131. <https://doi.org/10.1016/j.arabj.2020.07.017>
- [103] Olusegun, S. J.; Freitas, E. T.; Lara, L. R.; Mohallem, N. D. Synergistic effect of a spinel ferrite on the adsorption capacity of nano bio-silica for the removal of methylene blue. *Environ. Technol.* **2021**, *42*, 2163–2176. <https://doi.org/10.1080/09593330.2019.1694083>
- [104] Altıntug, E.; Altundag, H.; Tuzen, M.; Sari, A. Effective removal of methylene blue from aqueous solutions using magnetic loaded activated carbon as novel adsorbent. *Chem. Eng. Res. Des.* **2017**, *122*, 151–163. <https://doi.org/10.1016/j.cherd.2017.03.035>
- [105] Zuhara, S.; Pradhan, S.; Zakaria, Y.; Shetty, A. R.; McKay, G. Removal of methylene blue from water using magnetic GTL-derived biosolids: Study of adsorption isotherms and kinetic models. *Molecules* **2023**, *28*, 1511. <https://doi.org/10.3390/molecules28031511>
- [106] Jia, Z.; Wu, L.; Zhang, D.; Han, C.; Li, M.; Wei, R. Adsorption behaviors of magnetic carbon derived from wood tar waste for removal of methylene blue dye. *Diamond Relat. Mater.* **2022**, *130*, 109408. <https://doi.org/10.1016/j.diamond.2022.109408>
- [107] Arancibia-Miranda, N.; Baltazar, S. E.; García, A.; Muñoz-Lira, D.; Sepúlveda, P.; Rubio, M. A.; Altbir, D. Nanoscale zero valent supported by zeolite and montmorillonite: template effect of the removal of lead ion from an aqueous solution. *J. Hazard. Mater.* **2016**, *301*, 371–380. <https://doi.org/10.1016/j.jhazmat.2015.09.007>
- [108] Xu, P.; Zeng, G. M.; Huang, D. L.; Feng, C. L.; Hu, S.; Zhao, M. H.; Lai, C.; Wei Z.; Huang, C.; Xie, G. X. et al. Use of iron oxide nanomaterials in wastewater treatment: a review. *Sci. Total Environ.* **2012**, *424*, 1–10. <https://doi.org/10.1016/j.scitotenv.2012.02.023>
- [109] Yang, X.; Wan, Y.; Zheng, Y.; He, F.; Yu, Z.; Huang, J.; Wang, H.; Ok, Y. S.; Jiang, Y.; Gao, B. Surface functional groups of carbon-based adsorbents and their roles in the removal of heavy metals from aqueous solutions: a critical review. *Chem. Eng. J.* **2019**, *366*, 608–621. <https://doi.org/10.1016/j.cej.2019.02.119>
- [110] Jafari Kang, A.; Baghdadi, M.; Pardakhti, A. Removal of cadmium and lead from aqueous solutions by magnetic acid-treated activated carbon nanocomposite. *Desalin. Water Treat.* **2016**, *57*, 18782–18798. <https://doi.org/10.1080/19443994.2015.1095123>
- [111] Huong, P. T. L.; Lan, H.; An, T. T.; Van Quy, N.; Tuan, P. A.; Alonso, J.; Phan, M. H.; Le, A. T. Magnetic iron oxide-carbon nanocomposites: Impacts of carbon coating on the As (V) adsorption and inductive heating responses. *J. Alloys Compd.* **2018**, *739*, 139–148. <https://doi.org/10.1016/j.jallcom.2017.12.178>
- [112] Chen, M.; Shao, L. L.; Li, J. J.; Pei, W. J.; Chen, M. K.; Xie, X. H. One-step hydrothermal synthesis of hydrophilic Fe<sub>3</sub>O<sub>4</sub>/carbon



- composites and their application in removing toxic chemicals. *RSC Adv.* **2016**, *6*, 35228–35238. <https://doi.org/10.1039/c6ra01408a>
- [113] Zhang, J.; Zhai, S.; Li, S.; Xiao, Z.; Song, Y.; An, Q.; Tian, G. Pb (II) removal of Fe<sub>3</sub>O<sub>4</sub>@ SiO<sub>2</sub>-NH<sub>2</sub> core-shell nanomaterials prepared via a controllable sol-gel process. *Chem. Eng. J.* **2013**, *215*, 461–471. <https://doi.org/10.1016/j.cej.2012.11.043>
- [114] Ren, Y.; Abbood, H. A.; He, F.; Peng, H.; Huang, K. Magnetic EDTA-modified chitosan/SiO<sub>2</sub>/ Fe<sub>3</sub>O<sub>4</sub> adsorbent: preparation, characterization, and application in heavy metal adsorption. *Chem. Eng. J.* **2013**, *226*, 300–311. <https://doi.org/10.1016/j.cej.2013.04.059>
- [115] Gutha, Y.; Munagapati, V. S. Removal of Pb (II) ions by using magnetic chitosan-4-(pyridin-2-ylimino) methyl benzaldehyde Schiff's base. *Int. J. Biol. Macromol.* **2016**, *93*, 408–417. <https://doi.org/10.1016/j.ijbiomac.2016.08.084>
- [116] Cui, L.; Wang, Y.; Gao, L.; Hu, L.; Yan, L.; Wei, Q.; Du, B. EDTA functionalized magnetic graphene oxide for removal of Pb (II), Hg (II) and Cu (II) in water treatment: adsorption mechanism and separation property. *Chem. Eng. J.* **2015**, *281*, 1–10. <https://doi.org/10.1016/j.cej.2015.06.043>
- [117] Zhao, D.; Gao, X.; Wu, C.; Xie, R.; Feng, S.; Chen, C. Facile preparation of amino functionalized graphene oxide decorated with Fe<sub>3</sub>O<sub>4</sub> nanoparticles for the adsorption of Cr (VI). *Appl. Surf. Sci.* **2016**, *384*, 1–9. <https://doi.org/10.1016/j.apsusc.2016.05.022>
- [118] Hosseinzadeh, H.; Ramin, S. Effective removal of copper from aqueous solutions by modified magnetic chitosan/graphene oxide nanocomposites. *Int. J. Biol. Macromol.* **2018**, *113*, 859–868. <https://doi.org/10.1016/j.ijbiomac.2018.03.028>
- [119] Pipiška, M.; Zardňanská, S.; Horník, M.; Ďuriška, L.; Holub, M.; Šafařík, I. Magnetically functionalized moss biomass as biosorbent for efficient Co<sup>2+</sup> ions and thioflavin T removal. *Materials* **2020**, *13*, 3619. <https://doi.org/10.3390/ma13163619>

Received: March 18, 2024 / Revised: April 20, 2024 / Accepted: May 02, 2024

## МАГНІТОЧУТЛИВІ НАНОКОМПЗИТИ НА ВУГЛЕЦЕВІЙ ОСНОВІ ДЛЯ ОЧИЩЕННЯ СТІЧНИХ ВОД ВІД БАРВНИКІВ І ВАЖКИХ МЕТАЛІВ: ОГЛЯД

**Анотація.** Проаналізовано методи очищення стічних вод від іонів важких металів і барвників, показано ключові переваги порошкових магніточутливих вуглецевих нанокмпозитів як адсорбентів. Розглянуто методи вибору та підготовки сировини й активаторів для синтезу таких нанокмпозитів, проаналізовано методики синтезу нанокмпозитів. Описано властивості, моделювання кінетики й ізотерм адсорбції, ефективність застосування магнітних вуглецевих нанокмпозитів для очищення стічних вод від барвників і важких металів.

**Ключові слова:** адсорбція, вуглецевий нанокмпозит, магніточутливий адсорбент, очищення стічних вод, важкі метали, барвники.